

Vision Based 3-D Position Control for a Robot Arm

Cheng-Hao Huang¹, Chi-Sheng Hsu¹, Po-Chien Tsai¹, Rong-Jyue Wang², and Wen-June Wang^{1*}, *Fellow, IEEE*

¹Department of Electrical Engineering, National Central University, Jhongli, Taiwan

²Department of Electronic Engineering, National Formosa University, Huwei, Taiwan

wjwang@ee.ncu.edu.tw

Abstract—This paper presents a 3-D position control for a robot arm. The system contains a fabricated robot arm, a pair of charge-coupled device (CCD) cameras, and a computer. The inverse kinematics (IK) concept is utilized to manipulate the robot arm. The two-CCD vision geometry is utilized to measure the practical 3-D position of the robot arm's tip. Furthermore, a fuzzy position error compensator is added to adjust the target position for the IK technique such that the position accuracy can be guaranteed. The experimental results demonstrate that the robot arm can position its tip at the desired position accurately.

Keywords—robot arm, 3-D position control, fuzzy control, charge-coupled device (CCD) geometry

I. INTRODUCTION

Previous literatures regarding the robot arm motion control are reported as follows. Furuta *et al.* [1] proposed the dynamic equation of a robot arm. Based on sensor signal feedback, a PID control is designed for the arm to achieve the desired position. The papers [2], [3] established a simulation system of the robot arm such that the coordinates of each joint can be computed by the simulation system. Thus, the arm can be controlled to track an assigned trajectory. Using Mitsubishi PA-10 robot arm platform, the paper [4] proposed a concept of a harmonic drive model to investigate the gravity and material influence to robot arm. Then the robot arm is controlled to track a desired trajectory and the motion error is analyzed. In [5], a two-link robot arm is controlled by a fuzzy sliding mode controller in which the parameters are adjusted by fuzzy-neural techniques. Furthermore, the robot arm system in [6] is designed to implement the elevator buttons pushing behavior by using inverse kinematics (IK) technique. The thesis [13] uses inverse and forward kinematics to derive the dynamic equation of the robot arm, and then presents the analysis and simulation.

Recently, the three-dimension (3-D) vision systems for robot applications have been popularly studied. Baek and Lee [7] used two cameras and one laser sensor to recognize the elevator door and to determine its depth distance. Okada *et al.* [8] used multi-sensors for the 3-D position measurement. Winkelbach *et al.* [9] combined one camera with one range sensor to find the 3-D coordinate position of the target. Hsu [14] used one camera to achieve the vision-guided pose control for mobile robots. Yeh [15] used two cameras to capture the object features and to measure the target position.

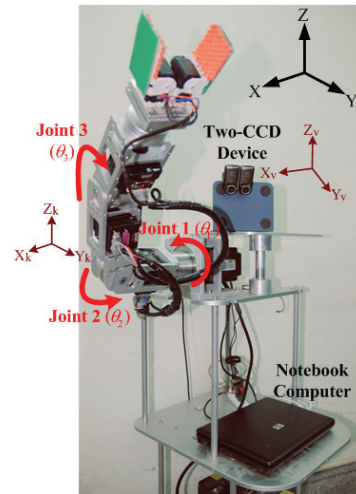


Figure 1. The robot arm system.

In this paper, a two-link robot arm system is fabricated with a two-charge-coupled device (CCD) vision system. The IK concept is utilized to manipulate the robot arm. The two-CCD vision geometry is utilized to measure the 3-D position of the robot arm's tip. Moreover, a fuzzy position error compensator is presented to adjust the target position for the IK technique. The 3-D position accuracy is therefore improved. An experiment is given in the final to demonstrate the feasibility of the proposed robot arm system.

II. SYSTEM DESCRIPTION

This section introduces the robot arm system which is designed to implement the 3-D position motion. Figure 1 shows a photograph of the robot arm system. The whole system mainly includes a fabricated robot arm, a two-CCD vision device, and a computer as the control center.

The robot arm consists of several servo motors with metal connections. Two main links with three joints are considered in the 3-D motion control for the robot arm. The Joint 1 is for the shoulder rotation, the Joint 2 is for the lifting movement, and the Joint 3 is for the elbow bending. The robot arm's tip is pasted by green patterns for the convenience of image processing. In the robot arm, each servo motor is combined with a speed-reducer gearbox to increase the rotary torque. All

This work was supported by the National Science Council, Taiwan, under the Grant NSC 98-2221-E-008-118-MY3 and NSC 99-2628-E-150-046.

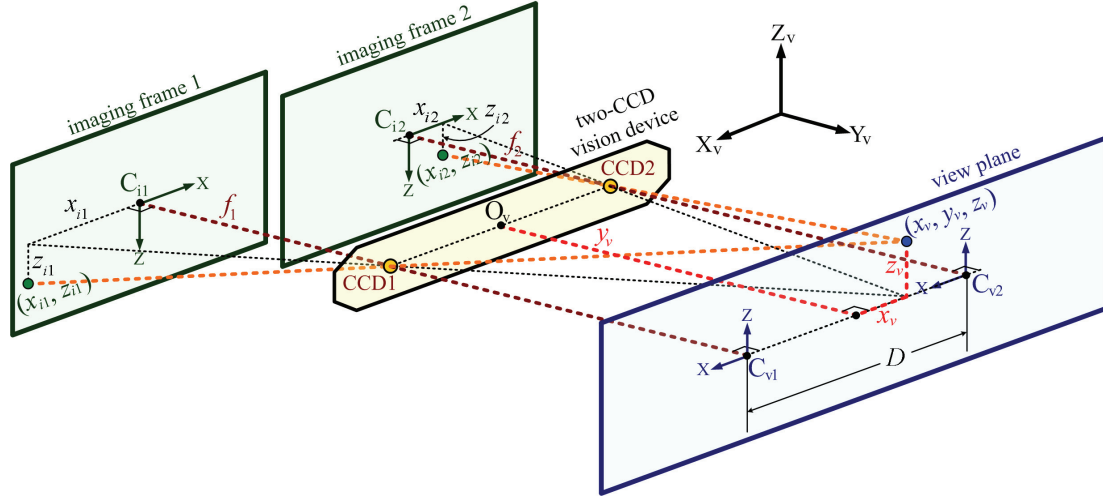


Figure 2. Two-CCD vision geometry.

the servo motors are controlled by serial RS-232 command signals from the computer.

The vision capability is the sensory feedback of the robot arm system for the sake of position control. Two CCD webcams (Logitech C905) are parallelly arranged as a two-CCD vision device on the top platform. Generally, the target point can be captured in a pair of spatial images. The 3-D position measurement of the robot arm can be obtained by the two-CCD vision geometry. As for the CCD webcam specification, the maximum resolution of each captured image is 640 x 320 pixels and the capturing rate is 30 frames per second.

The control center of the robot arm system is a notebook computer with an Intel Core 2 Duo 2.4 GHz CPU and 2 GB random-access memory (RAM). The computer is employed to conduct the two-CCD image processing, the pattern recognition, the vision geometric calculation and position measurement, and the motion control for the robot arm system. Herein, Borland C++ Builder is the software solution for the computer to implement the complete process.

III. TWO-CCD VISION MEASUREMENT

The premier task in this paper is to control the robot arm to reach the target position successfully. Hence, the main concern is to measure the 3-D position of the robot arm's tip by using two 2-D imaging frames of the two-CCD vision device. Before the requisite geometric analysis, three 3-D configurations are defined in the working space. The first is the world configuration $[X, Y, Z]^T$, the second is the vision configuration $[X_v, Y_v, Z_v]^T$ for the CCD measurement, and the last is the kinematics configuration $[X_k, Y_k, Z_k]^T$ for the motion control design of the robot arm (see Fig. 1).

A. Two-CCD Vision Geometry

A two-CCD vision system is presented to achieve the 3-D position measurement for the robot arm. Assume that two CCD

cameras are horizontally and parallelly set up to capture a perpendicular view plane, and a pair of different imaging frames can be obtained for further geometric analysis. Figure 2 illustrates the schematic diagram of the two-CCD vision geometry for the 3-D position measurement, in which f_1 and f_2 are focal lengths of CCD1 and CCD2, respectively, and a separated distance D exists between CCD1 and CCD2. Moreover, C_{i1} and C_{i2} are the centers of imaging frames 1 and 2, respectively. Then C_{v1} and C_{v2} denote the CCD1's and CCD2's optical points on the view plane, respectively. Overall, the midpoint O_v between CCD1 and CCD2 is the origin of the vision configuration $[X_v, Y_v, Z_v]^T$.

The 3-D position measurement is to obtain the robot arm's tip position (x_v, y_v, z_v) by using the two 2-D vectors (x_{i1}, z_{i1}) and (x_{i2}, z_{i2}) which are the reflected coordinates on the imaging frames 1 and 2, respectively. With the benefit of Fig. 2, the photographic distance y_v is firstly derived as (1a). Then the values of x_v and z_v can be obtained as (1b) and (1c), respectively [11].

$$y_v = \frac{D}{\frac{|x_{i1}|}{f_1} + \frac{|x_{i2}|}{f_2}} \quad (1a)$$

$$x_v = \frac{1}{2} \cdot \left(\frac{x_{i1}}{f_1} + \frac{x_{i2}}{f_2} \right) \cdot y_v \quad (1b)$$

$$z_v = \frac{z_{i1}}{f_1} \cdot y_v \quad \left(\text{or } z_v = \frac{z_{i2}}{f_2} \cdot y_v \right) \quad (1c)$$

Consequently, the 3-D position measurement of (x_v, y_v, z_v) for the robot arm is achieved.

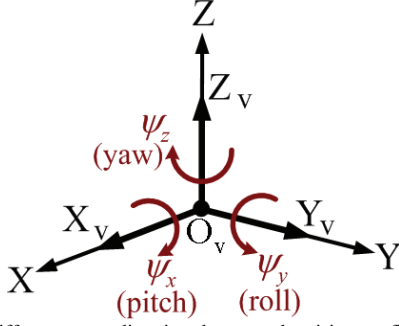


Figure 3. Different rotary directions between the vision configuration and the world configuration.

B. Configuration Transformation

In the working space, O_v is equally assigned as the origin of the world configuration $[X, Y, Z]^T$. As depicted in Fig. 3, the difference between the vision configuration and the world configuration is a three-phase angle which can be divided into a pitch angle ψ_x , a roll angle ψ_y , and a yaw angle ψ_z . Herein, the three-phase rotation matrices can be added to transform the 3-D coordinate from the vision configuration to the world configuration. Consequently, the desired 3-D position (x_v, y_v, z_v) in vision configuration can be described by the following resulting world coordinate (x, y, z) .

$$\begin{bmatrix} x \\ y \\ z \end{bmatrix} = \begin{bmatrix} \cos \psi_z & \sin \psi_z & 0 \\ -\sin \psi_z & \cos \psi_z & 0 \\ 0 & 0 & 1 \end{bmatrix} \begin{bmatrix} \cos \psi_y & 0 & \sin \psi_y \\ 0 & 1 & 0 \\ -\sin \psi_y & 0 & \cos \psi_y \end{bmatrix} \begin{bmatrix} 1 & 0 & 0 \\ 0 & \cos \psi_x & \sin \psi_x \\ 0 & -\sin \psi_x & \cos \psi_x \end{bmatrix} \begin{bmatrix} x_v \\ y_v \\ z_v \end{bmatrix} \quad (2)$$

IV. POSITION CONTROL DESIGN

A. Motion Control

The IK is a well-known technique employed to manipulate a robot arm. Figure 4 illustrates the kinematics configuration of the robot arm, where O_k is the origin of the kinematics configuration $[X_k, Y_k, Z_k]^T$, Q is the elbow node, and (x_k, y_k, z_k) is the robot arm tip's position. The lengths of the links 1 and 2 are denoted as d_1 and d_2 , respectively. Thus, the two links with the three joints $(\theta_1, \theta_2, \theta_3)$ are established such that the robot arm can possess the 3-D motion flexibility (see Fig. 1 and Fig. 4). Let $L = \sqrt{x_k^2 + y_k^2 + z_k^2}$, $L_{yz} = \sqrt{y_k^2 + z_k^2}$, the mapping joint angles $(\theta_1, \theta_2, \theta_3)$ for the robot arm can be obtained by geometric derivations (3a)–(3c) [12].

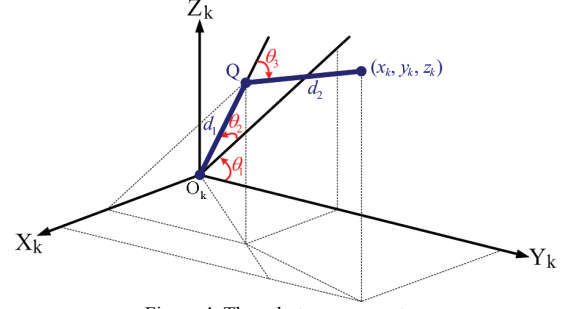


Figure 4. The robot arm geometry.

$$\theta_3 = \pi - \cos^{-1} \left(\frac{d_1^2 + d_2^2 - L^2}{2d_1d_2} \right), \text{ where } 0 \leq \theta_3 \leq \pi/2 \quad (3a)$$

$$\theta_2 = \sin^{-1} \left(\frac{x_k}{d_1 + d_2 \cos \theta_3} \right), \text{ where } 0 \leq \theta_2 \leq \pi/2 \quad (3b)$$

$$\theta_1 = \cos^{-1} \left(\frac{L_{yz}^2 + ((d_1 + d_2 \cos \theta_3) \cos \theta_2)^2 - (d_2 \sin \theta_2)^2}{2L_{yz}((d_1 + d_2 \cos \theta_3) \cos \theta_2)} \right) + \sin^{-1} \left(\frac{z_k}{L_{yz}} \right), \text{ where } 0 \leq \theta_1 \leq \pi/2 \quad (3c)$$

Then transform (3a)–(3c) to the motor control signals, the robot arm's tip can be expected to reach the target position (x_k, y_k, z_k) . Meanwhile, the shifting relationship between the kinematics configuration and the world configuration can be represented as follows.

$$\begin{bmatrix} x \\ y \\ z \end{bmatrix} = \begin{bmatrix} x_k \\ y_k \\ z_k \end{bmatrix} + (O_k - O_v) \quad (4)$$

Practically, the motor backlash problems and the hardware uncertainties affect the 3-D position accuracy. The two-CCD measurement is suggested to determine the position accuracy and a fuzzy position error compensator is added to improve the open-loop IK control technique.

B. Fuzzy Position Error Compensator

Generally, if the desired 3-D position of the robot arm's tip is assigned as $P_d(x_d, y_d, z_d)$, the target position $P_t(x_t, y_t, z_t)$ of IK should be the same as P_d , i.e., $P_t = P_d$. By using the IK technique, the robot arm's tip is expected to reach the target position P_t . In addition, the practical position $P(x, y, z)$ can be measured by the two-CCD vision system. Herein, the position error is defined as

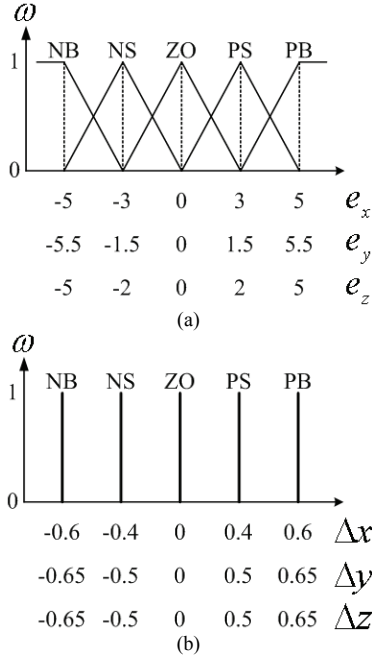


Figure 5. (a) Membership functions of e_k .
(b) Membership functions of Δk .

$$\begin{aligned} \mathbf{e} &= \mathbf{P} - \mathbf{P}_d \\ &= (x - x_d, y - y_d, z - z_d) \\ &= (e_x, e_y, e_z), \end{aligned} \quad (5)$$

where e_k denotes the error on the k -axis, and $k = x, y, z$. The fuzzy position error compensator is a fuzzy rule base (FRB) (6) in which the antecedent is e_k and the consequent is the compensation step Δk for adjusting the target position \mathbf{P}_t . Both are decomposed into five fuzzy sets, including NB (negative big), NS (negative small), ZO (zero), PS (positive small), and PB (positive big).

$$\text{FRB:} \begin{cases} \text{Rule1: If } e_k \text{ is NB, then } \Delta k \text{ is NB;} \\ \text{Rule2: If } e_k \text{ is NS, then } \Delta k \text{ is NS;} \\ \text{Rule3: If } e_k \text{ is ZO, then } \Delta k \text{ is ZO;} \\ \text{Rule4: If } e_k \text{ is PS, then } \Delta k \text{ is PS;} \\ \text{Rule5: If } e_k \text{ is PB, then } \Delta k \text{ is PB,} \end{cases} \quad (k = x, y, z) \quad (6)$$

Figure 5 shows the membership functions of e_k and Δk . The defuzzification strategy is implemented by the weighted average method [10].

$$\Delta k = \sum_{r=1}^5 \omega^r(e_k) \cdot u_k^r, \quad (k = x, y, z) \quad (7)$$

where $\omega^r(e_k)$ is the fired weight of r th rule, u_k^r is the support of r th consequent fuzzy set, and $\sum_{r=1}^5 \omega^r(e_k) = 1$.

C. Position Control Design

Summarize the IK kinematics technique and the fuzzy position error compensator, the position control procedures are described as the following steps.

Step 1: Let the initial target position be the desired position, i.e., $\mathbf{P}_t^{(0)} = \mathbf{P}_d$.

Step 2: By using the IK method, the robot arm's tip is controlled to approach \mathbf{P}_t .

Step 3: Use the two-CCD vision system to measure the current position \mathbf{P} .

Step 4: Evaluate the position error $\mathbf{e} = \mathbf{P} - \mathbf{P}_d$. If $\|\mathbf{e}\| \leq \rho$ (error threshold), then the control is terminated. Otherwise, continue to Step 5.

Step 5: Using the FRB (6) and the defuzzification (7) to determine the compensation steps of target position Δk , ($k = x, y, z$).

Step 6: Update the target position as

$$\mathbf{P}_t^{(i+1)} = (x_t^{(i)} + \Delta x, y_t^{(i)} + \Delta y, z_t^{(i)} + \Delta z) \text{ and go to Step 2.}$$

Here, i denotes the control iteration count. Based on the mentioned six steps, the 3-D position control is completed.

V. EXPERIMENTAL RESULTS

An experiment is given to verify the feasibility of the proposed 3-D position control for the established robot arm (Fig. 1). Figure 6 demonstrates the experimental results. The rotation difference between $[X_v, Y_v, Z_v]^T$ and $[X, Y, Z]^T$ is $(\psi_x, \psi_y, \psi_z) = (27^\circ, 0^\circ, 60^\circ)$. The desired position is set as $\mathbf{P}_d(4.8, 41.2, -7.5)$, and the initial target position for IK is therefore set as $\mathbf{P}_t^{(0)} = \mathbf{P}_d$. The terminated condition is predefined as $\|\mathbf{e}\| \leq \rho = 1.5$ which is the accuracy requirement. In Fig. 6, the robot arm is controlled to reach $\mathbf{P}^{(4)}(3.9, 41.4, -7)$. The position error is reduced to be $\|\mathbf{e}\| \approx 1.05 \leq \rho$ that satisfies the accuracy requirement.

VI. CONCLUSION

This paper has implemented the 3-D position control for a robot arm. The presented methods include the two-CCD vision measurement, the IK technique, and the fuzzy position error compensator, which are collocated to achieve the position behavior. Through the practical experiments, the proposed position control has been shown useful for the real robot arm.

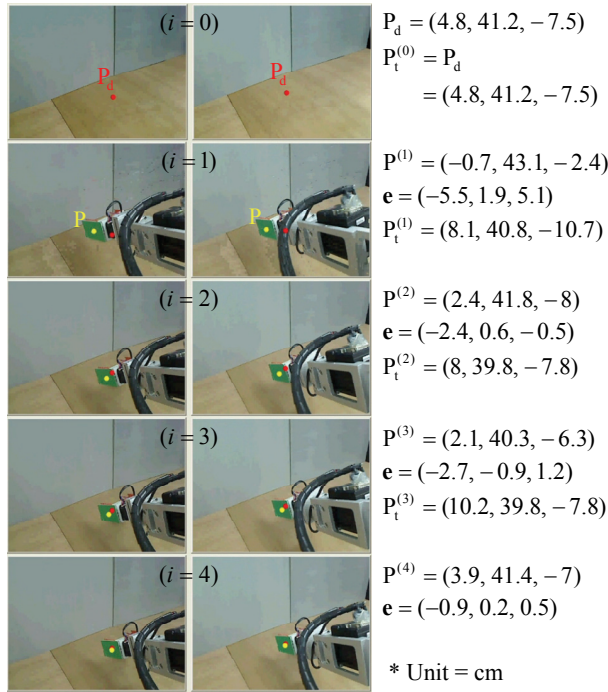


Figure 6. Experimental results of the position control for the robot arm.

ACKNOWLEDGMENT

This work is supported by the National Science Council, Taiwan, under the Grant NSC 98-2221-E-008-118-MY3 and NSC 99-2628-E-150-046.

REFERENCES

- [1] K. Furuta, K. Kosuge, and N. Mukai, "Control of articulated robot arm with sensory feedback: Laser beam tracking system," *IEEE Trans. Ind. Electron.*, vol. 35, no. 1, pp. 31–39, Feb. 1988.
- [2] R. B. White, R. K. Read, M. W. Koch, and R. J. Schilling, "A graphics simulator for a robotic arm," *IEEE Trans. Educ.*, vol. 32, no. 4, pp. 417–429, Nov. 1989.
- [3] S. R. Munasinghe, M. Nakamura, S. Goto, and N. Kyura, "Optimum contouring of industrial robot arms under assigned velocity and torque constraints," *IEEE Trans. Syst. Man Cybern. Part C-Appl. Rev.*, vol. 31, no. 2, pp. 159–167, May 2001.
- [4] C. W. Kennedy and J. P. Desai, "Modeling and control of the Mitsubishi PA-10 robot arm harmonic drive system," *IEEE-ASME Trans. Mechatron.*, vol. 10, no. 3, pp. 263–274, Jun. 2005.
- [5] M. Ö. Efe, "Fractional fuzzy adaptive sliding-mode control of a 2-DOF direct-drive robot arm," *IEEE Trans. Syst. Man Cybern. Part B- Cybern.*, vol. 38, no. 6, pp. 1561–1570, Dec. 2008.
- [6] W.-J. Wang, C.-H. Huang, I.-H. Lai, and H.-C. Chen, "A robot arm for pushing elevator buttons," in *SICE Annual Conference 2010*, Taipei, Taiwan, Aug. 2010, pp. 1844–1848.
- [7] J.-Y. Baek and M.-C. Lee, "A study on detecting elevator entrance door using stereo vision in multi floor environment," in *Proc. ICROS-SICE Int. Joint Conf. 2009*, Fukuoka, Japan, Aug. 2009, pp. 1370–1373.
- [8] K. Okada, M. Kojima, S. Tokutsu, T. Maki, Y. Mori, and M. Inaba, "Multi-cue 3D object recognition in knowledge-based vision-guided humanoid robot system," in *Proc. 2007 IEEE/RSJ Int. Conf. Intell. Robot. Syst.*, CA, USA, Oct. 2007, pp. 3217–3222.
- [9] S. Winkelbach, S. Molkenstruck, and F. M. Wahl, "Low-cost laser range scanner and fast surface registration approach," in *Proc. DAGM Symp. Pattern Recognit.*, Berlin, Germany, Sep. 2006.
- [10] T.-H. S. Li, S.-J. Chang, and W. Tong, "Fuzzy target tracking control of autonomous mobile robots by using infrared sensors," *IEEE Trans. Fuzzy Syst.*, vol. 12, no. 4, pp. 491–501, Aug. 2004.
- [11] C.-S. Hsu, "Two-CCD based 3-D position measurement," M.S. thesis, Dept. Electrical Engineering, National Central University, Taiwan, 2011. (in Chinese).
- [12] P.-C. Tsai, "Inverse kinematics based motion control for a two-link manipulator," M.S. thesis, Dept. Electrical Engineering, National Central University, Taiwan, 2011. (in Chinese).
- [13] P.-C. Hwang, "Dynamic simulation and analysis of the robot arm in minimal invasive surgery," M.S. thesis, Dept. Mechanical Engineering, National Central University, Taiwan, 2006. (in Chinese).
- [14] M.-S. Hsu, "Pose control of mobile robots for vision-guided material," M.S. thesis, Dept. Mechanical Engineering, National Cheng Kung University, Taiwan, 2002. (in Chinese).
- [15] N.-H. Yeh, "Grasping control of a mobile manipulator," M.S. thesis, Dept. Electrical and Control Engineering, National Chiao Tung University, Taiwan, 2006. (in Chinese).